Parameter Identification of the Nonlinear Double-Capacitor Model for Lithium-Ion Batteries: From the Wiener Perspective

Ning Tian, Huazhen Fang and Yebin Wang

***Abstract*— Battery parameter identification is emerging as an important topic due to the increasing use of battery energy storage. This paper studies parameter identification for the nonlinear double-capacitor (NDC) model for lithium-ion batteries, which is a new equivalent circuit model developed in the authors' previous work [1]. It is noticed that the NDC model has a structure similar to the Wiener system. From this Wiener perspective, this work builds a parameter identification approach for this model upon the well-known maximum *a posteriori* (MAP) estimation. The purpose of using MAP is to overcome the nonconvexity and local minima that can cause unphysical parameter estimates. A quasi-Newton-based method is utilized to accomplish the involved optimization procedure numerically. The proposed approach is the first one that we aware of exploits MAP for Wiener system identification. It also demonstrates significant effectiveness for accurate identification of the NDC model as validated through experiments.**

I. Introduction

Battery modeling and parameter identification are of foundational importance for model-based battery management to ensure the performance, safety and life of various battery systems. Despite a growing amount of research, many new challenges continue to arise due to an ever-increasing demand for better accuracy, efficiency and availability of battery models. In this context, this paper contributes a study of parameter identification for the nonlinear double-capacitor (NDC) model, an equivalent circuit model for lithium-ion batteries (LiBs) proposed in our previous work [1]. Our study connects the Wiener system identification with the NDC model as the latter demonstrates a Wiener-type structure. We propose a parameter estimation approach that enhances existing Wiener identification methods and proves to be effective for the NDC model.

Literature Review. Battery parameter identification has attracted considerable attention in recent years. The current literature can be divided into two main categories, experiment-based and data-based. The first category conducts experiments of charging, discharging or electrochemical impedance spectroscopy (EIS) and utilizes the experimental data to directly determine a model's parameters. It is pointed out in [2–4] that the transient voltage responses under constant- or pulse-current charging/discharging can expose the resistance, capacitance and time constant parameters of the well-known Thevenin's model. The relationship between the state of charge (SoC) and open-circuit voltage (OCV) greatly characterizes a battery's dynamics. It can be experimentally identified by charging or discharging a battery using a very small current [5], or alternatively, using a current of normal magnitude but intermittently (a sufficiently long rest period is applied between two discharging operations) [6; 7]. The EIS experiments have also been widely used to identify a battery's impedance properties [8–10]. While involving basic data analysis, these methods generally put emphasis on the design of experiments. By contrast, the second category seeks to deeply understand the model-data relationship and build sophisticated data-driven approaches to construct models from data. It can beneficially enable provably correct identification, even for complex models, in addition promising better use of data and convenient application. It is proposed in [11] to identify the Thevenin's model by solving a set of linear and polynomial equations. Another popular means is to formulate model-data fitting problems and solve them using least squares, instrumental variables or other optimization methods to estimate the parameters [12–18]. In [19; 20], a linear state-space model is formulated for batteries, and subspace identification is then performed to infer the system matrices. When more complex electrochemical models are considered, the identification usually involves large-size nonlinear nonconvex optimization problems. In this case, particle swarm optimization and genetic algorithms are often leveraged to search for the best parameter estimates [21–24]. Another topic of interest is optimal input design to maximize the parameter identifiability [25; 26].

Compared with the above studies, the NDC model presents a different yet intriguing challenge—it has a Wiener-type structure featuring a linear dynamic subsystem in cascade with a static nonlinear subsystem. Although our work in [1] provides a parameter estimation scheme, it is limited to only constant charging or discharging protocols. None of the existing methods is applicable here since they are designed for non-Wiener-type models. We are thus motivated to custom-develop an approach with an awareness of the NDC model's Wiener-like structure. Wiener system identification is an important subject in the area of system identification, which has seen a few methods proposed in the literature [27]. Among them, one of the most promising is based on the maximum likelihood (ML) estimation [28; 29]. However, the optimization procedure resulting from the ML formulation often suffers the issue of local minima, fundamentally blamed on the nonlinearity involved in the NDC model. If not addressed, this problem can easily lead to parameter estimates physically meaningless and useless when one applies the ML method to identifying the NDC model.

N. Tian and H. Fang are with the Department of Mechanical Engineering, University of Kansas, Lawrence, KS, 66045 USA {ning.tian@ku.edu, fang@ku.edu}.

Y. Wang is with the Mitsubishi Electric Research Laboratories, Cambridge, MA, 02139 USA {yebinwang@merl.com}.

Statement of Contributions. Focused on identification, this work offers three contri propose to enable Wiener system identif maximum *a posteriori* (MAP) estimation. (MAP incorporates into the estimation desig tion of the unknown parameters, which rep information or prior knowledge and ca parameter search toward a physically reas space. Second, based on the above notion, develop an MAP-based parameter identifica the NDC model. The proposed approach ca model parameters in just one shot and a arbitrary current profiles. Finally, we evalu using experiments, well validating its effic

Organization. The rest of the paper is lows. Section II reveals the Wiener-type str the NDC model. Inspired by Wiener system identification, Section III develops a new MAP-based parameter estimation approach to identify the NDC model. Section IV offers experimental validation to assess the proposed approach. Finally, some concluding remarks are gathered in Section V.

II. The NDC Model

This section introduces the NDC model and further unveils its inherent Wiener-type architecture.

The NDC model is schematically shown in Figure 1. It is an extension of a linear double-capacitor model to account for a battery's nonlinear phenomena [1]. Its first main part is two R-C circuits, i.e., C_b-R_b and C_s-R_s, which are configured in parallel. They are designed to imitate a battery's electrode. Specifically, C_b-R_b is analogous to the electrode's bulk inner part, and C_s-R_s corresponds to the surface region. The charge is stored in and migrates between C_b and C_s. This hence implies $C_b \gg C_s$ and $R_b \gg R_s$. The second part consists of a voltage source U and an internal resistance R_0. Here, U is an analog to the OCV and based on a nonlinear mapping of V_s, i.e., $U = h(V_s)$. In addition, R_0 is included to mimic the electrolyte resistance. It is shown in [1] that this model provides excellent predictive capability for a battery's voltage behavior.

The dynamics of the NDC model can be characterized by the following state-space model:

$$\begin{cases} \begin{bmatrix} \dot{V}_b(t) \\ \dot{V}_s(t) \end{bmatrix} = A \begin{bmatrix} V_b(t) \\ V_s(t) \end{bmatrix} + BI(t), & \text{(1a)} \\ V(t) = h(V_s(t)) + R_0 I(t), & \text{(1b)} \end{cases}$$

where V_b and V_s are the voltages across C_b and C_s, respectively, I the current applied for charging ($I > 0$) or discharging ($I < 0$), V the terminal voltage, and

$$A = \begin{bmatrix} -\frac{1}{C_b(R_b+R_s)} & \frac{1}{C_b(R_b+R_s)} \\ \frac{1}{C_s(R_b+R_s)} & -\frac{1}{C_s(R_b+R_s)} \end{bmatrix}, \; B = \begin{bmatrix} \frac{R_s}{C_b(R_b+R_s)} \\ \frac{R_b}{C_s(R_b+R_s)} \end{bmatrix}.$$

Besides, we parameterize $h(V_s)$ as a fifth-order polynomial:

$$h(V_s) = \beta_0 + \beta_1 V_s + \beta_2 V_s^2 + \beta_3 V_s^3 + \beta_4 V_s^4 + \beta_5 V_s^5,$$

where β_i for $i = 0, 1, \ldots, 5$ are coefficients. Note that V_b and V_s should be set to belong to an interval $[\underline{V}_s, \overline{V}_s]$, and

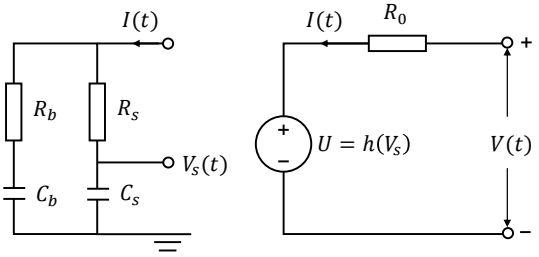

Fig. 1: Diagram of a nonlinear double-capacitor model.

for simplicity we let $\underline{V}_s = 0$ V and $\overline{V}_s = 1$ V. Then, $C_b + C_s$ corresponds to a battery's full capacity, $V_b = V_s = 1$ V for full charge (SoC $= 100\%$), and $V_b = V_s = 0$ V for full depletion (SoC $= 0\%$). In this work, we consider full discharging experiments to identify the model. That is, the initial V is $\overline{V}$ that corresponds to the voltage at full charge, and the discharging ends when V hits the cut-off threshold $\underline{V}$. Then, we can obtain $\beta_0 = \underline{V}$ and $\sum_{i=0}^{5} \beta_i = \overline{V}$. Furthermore, it can also be easily derived that OCV $= h(\text{SoC})$ holds [1]. Looking further at the NDC model, we can see that it has a structure akin to a Wiener system—the parallel R-C circuits constitute a linear dynamic subsystem, and cascaded with it is a static nonlinear mapping. Next, we convert (1) to a discrete-time Wiener-type formulation.

Applying zero-order-hold discretization to (1a) and deriving the transfer-function form, we have

$$V_s(t) = G_1(q)I(t) + G_2(q)V_s(0), \quad (2)$$

where

$$G_1(q) = \frac{\alpha_1 q^{-1} + \alpha_2 q^{-2}}{1 - (1+\alpha_3)q^{-1} + \alpha_3 q^{-2}},$$
$$G_2(q) = \frac{1}{1 - q^{-1}},$$

with

$$\alpha_1 = \frac{A_{21}B_{11} + A_{12}B_{21}}{A_{12} + A_{21}}\Delta t - \frac{A_{21}B_{11} - A_{21}B_{21}}{(A_{12} + A_{21})^2}(1 - \alpha_3),$$
$$\alpha_2 = -\frac{A_{21}B_{11} + A_{12}B_{21}}{A_{12} + A_{21}}\alpha_3 \Delta t + \frac{A_{21}B_{11} - A_{21}B_{21}}{(A_{12} + A_{21})^2}(1 - \alpha_3),$$
$$\alpha_3 = e^{-(A_{12}+A_{21})\Delta t}.$$

Here, q^{-1} is the backshift operator, i.e., $q^{-1}s(t) = s(t-1)$ for a signal $s(t)$, and Δt the sampling period. It should be noted that only three parameters, α_i for $i = 1, 2, 3$ appear in (2), though (1a) involves four physical parameters, C_b, C_s, R_b and R_s. Hence, there is a redundancy for the physical parameters, which implies unidentifiability. To fix this issue, we let $R_s = 0$ following [12], because of the relatively less important role of R_s. Then, one can find out that

$$\alpha_1 = \breve{\alpha}_1 + \breve{\alpha}_2,$$
$$\alpha_2 = -\breve{\alpha}_1\breve{\alpha}_3 - \breve{\alpha}_2,$$
$$\alpha_3 = \breve{\alpha}_3,$$

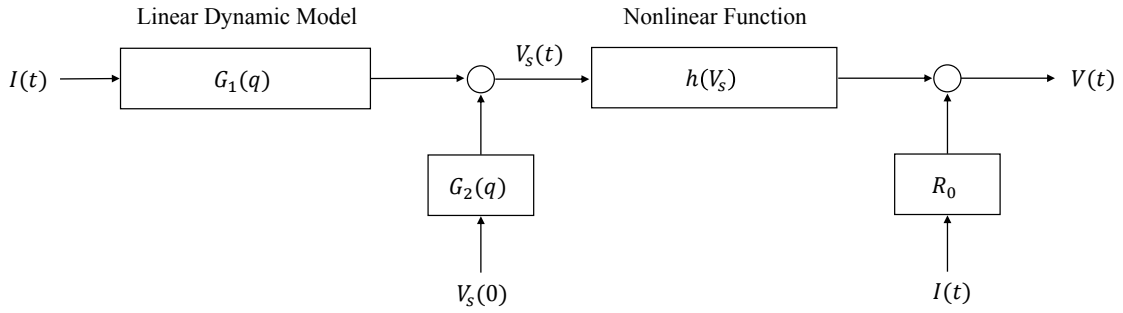

Fig. 2: The Wiener-type structure of the NDC model.

with

$$\breve{\alpha}_1 = \frac{\Delta t}{C_b + C_s},\ \breve{\alpha}_2 = \frac{R_b C_b^2\,(1-\breve{\alpha}_3)}{(C_b+C_s)^2},\ \breve{\alpha}_3 = e^{-\frac{C_b+C_s}{C_b C_s R_b}\Delta t}.$$

If $\breve{\alpha}_i$ for $i = 1, 2, 3$ are determined, we can easily reconstruct α_i for $i = 1, 2, 3$ as well as C_b, C_s and R_b as follows:

$$\begin{aligned} C_b &= \frac{\Delta t}{\breve{\alpha}_1} - C_s, \\ C_s &= \frac{\breve{\alpha}_1(1-\breve{\alpha}_3)\Delta t}{\breve{\alpha}_1(\breve{\alpha}_1 - \breve{\alpha}_1\breve{\alpha}_3 - \breve{\alpha}_2 \log \breve{\alpha}_3)}, \\ R_b &= -\frac{(\Delta t)^2}{C_b C_s \breve{\alpha}_1 \log \breve{\alpha}_3}. \end{aligned}$$

Finally, it is obvious that V is governed by

$$V(t) = h\left[G_1(q)I(t) + G_2(q)V_s(0)\right] + R_0 I(t). \tag{3}$$

With the above formulation, we have the block-oriented Wiener-type structure of the NDC model as depicted in Figure 2, in which the linear dynamic model $G_1(q)$ and the nonlinear function $h(V_s)$ are interconnected sequentially. Given this Wiener-type model, we wish to estimate all of its parameters simultaneously, including $\breve{\alpha}_i$ for $i = 1, 2, 3$, β_i for $i = 1, 2, \ldots, 4$ and R_0, from the I-V data.

III. Parameter Identification

We address the NDC parameter identification from the Wiener perspective in this section. We build the solution on Bayesian MAP estimation.

Before proceeding further, we pose the following model based on (3):

$$y(t) = V(\boldsymbol{\theta}; u(t)) + v(t), \tag{4}$$

where u is the input current I, y the measured voltage, v the measurement noise added to V and assumed to follow a Gaussian distribution $\mathcal{N}(0, \sigma)$, and

$$\begin{aligned} \boldsymbol{\theta} &= \begin{bmatrix} \breve{\alpha}_1 & \breve{\alpha}_2 & \breve{\alpha}_3 & \beta_1 & \beta_2 & \beta_3 & \beta_4 & R_0 \end{bmatrix}^\top, \\ V(\boldsymbol{\theta}; u(t)) &= h\left[G_1(q, \boldsymbol{\theta})u(t) + G_2(q)V_s(0), \boldsymbol{\theta}\right] + \theta_8 u(t). \end{aligned}$$

The input (current) and output (voltage) datasets are denoted as

$$\begin{aligned} \boldsymbol{u} &= \begin{bmatrix} u(t_1) & u(t_2) & \cdots & u(t_N) \end{bmatrix}^\top \in \mathbb{R}^{N\times 1}, \\ \boldsymbol{y} &= \begin{bmatrix} y(t_1) & y(t_2) & \cdots & y(t_N) \end{bmatrix}^\top \in \mathbb{R}^{N\times 1}, \end{aligned}$$

where N is the total number of sample instants. A combination of them is expressed as

$$\boldsymbol{Z} = \begin{bmatrix} \boldsymbol{u} & \boldsymbol{y} \end{bmatrix}.$$

An ML-based approach is developed in [28] to deal with Wiener system identification. If applied to (4), it leads to consideration of the following problem:

$$\hat{\boldsymbol{\theta}} = \arg\max_{\boldsymbol{\theta}} p(\boldsymbol{Z}|\boldsymbol{\theta}).$$

Following this line, one can derive a likelihood cost function and find out the parameter estimates to minimize it. However, this method can be vulnerable to the risk of getting stuck at local minima because of the nonconvexity issue resulting from the static nonlinear function $h(\cdot)$. This can cause unphysical estimates. While carefully selecting an initial guess is suggested as a means to alleviate this problem [30], it may still not be adequate.

To overcome this problem, we propose to perform MAP estimation as it incorporates some prior knowledge to help drive the parameter search toward a reasonable minimum point. Specifically, we consider maximizing the *a posteriori* probability distribution of $\boldsymbol{\theta}$ conditioned on $\boldsymbol{Z}$:

$$\hat{\boldsymbol{\theta}} = \arg\max_{\boldsymbol{\theta}} p(\boldsymbol{\theta}|\boldsymbol{Z}). \tag{5}$$

Using the Bayes' theorem, we have

$$p(\boldsymbol{\theta}|\boldsymbol{Z}) = \frac{p(\boldsymbol{Z}|\boldsymbol{\theta}) \cdot p(\boldsymbol{\theta})}{p(\boldsymbol{Z})} \propto p(\boldsymbol{Z}|\boldsymbol{\theta}) \cdot p(\boldsymbol{\theta}).$$

In above, $p(\boldsymbol{\theta})$ quantifies the prior information available about $\boldsymbol{\theta}$. A general way is to characterize it as a Gaussian random vector following the distribution $p(\boldsymbol{\theta}) \sim \mathcal{N}(\boldsymbol{m}, \boldsymbol{P})$. Based on (4), $p(\boldsymbol{y}|\boldsymbol{\theta}) \sim \mathcal{N}(\boldsymbol{V}(\boldsymbol{\theta}; \boldsymbol{u}), \boldsymbol{Q})$, where $\boldsymbol{Q} = \sigma \boldsymbol{I}$ and

$$\boldsymbol{V}(\boldsymbol{\theta}; \boldsymbol{u}) = \begin{bmatrix} V(\boldsymbol{\theta}; u(t_1)) & \cdots & V(\boldsymbol{\theta}; u(t_N)) \end{bmatrix}^\top.$$

It then follows that

$$p(\boldsymbol{Z}|\boldsymbol{\theta}) \cdot p(\boldsymbol{\theta}) \propto \exp\left(-\frac{1}{2} \left[\boldsymbol{y} - \boldsymbol{V}\left(\boldsymbol{\theta};\boldsymbol{u}\right)\right]^{\top} \boldsymbol{Q}^{-1} \left[\boldsymbol{y} - \boldsymbol{V}\left(\boldsymbol{\theta};\boldsymbol{u}\right)\right] \right) \cdot \exp\left(-\frac{1}{2} \left(\boldsymbol{\theta} - \boldsymbol{m}\right)^{\top} \boldsymbol{P}^{-1} \left(\boldsymbol{\theta} - \boldsymbol{m}\right) \right).$$

Considering the log-likelihood, the problem formulated in (5) can be expressed as

$$\hat{\boldsymbol{\theta}} = \arg\min_{\boldsymbol{\theta}} J(\boldsymbol{\theta}), \tag{6}$$

where

$$J(\boldsymbol{\theta}) = \frac{1}{2} \left[\boldsymbol{y} - \boldsymbol{V}\left(\boldsymbol{\theta};\boldsymbol{u}\right)\right]^{\top} \boldsymbol{Q}^{-1} \left[\boldsymbol{y} - \boldsymbol{V}\left(\boldsymbol{\theta};\boldsymbol{u}\right)\right] + \frac{1}{2} \left(\boldsymbol{\theta} - \boldsymbol{m}\right)^{\top} \boldsymbol{P}^{-1} \left(\boldsymbol{\theta} - \boldsymbol{m}\right).$$

One must resort to numerical optimization to solve (6). Here, we exploit a quasi-Newton method [31] and introduce it briefly in the following for the sake of completeness. This method is premised on iteratively updating the parameter estimate, i.e.,

$$\boldsymbol{\theta}_{k+1} = \boldsymbol{\theta}_k + \lambda_k \boldsymbol{s}_k.$$

Here, λ denotes the step size, and $\boldsymbol{s}_k$ the gradient-based search direction given by

$$\boldsymbol{s}_k = -\boldsymbol{B}_k \boldsymbol{g}_k,$$

where $\boldsymbol{B}_k \in \mathbb{R}^{8\times 8}$ is a positive definite matrix that approximates the Hessian matrix $\nabla^2 J\left(\boldsymbol{\theta}_k\right)$, and $\boldsymbol{g}_k = \nabla J\left(\boldsymbol{\theta}_k\right) \in \mathbb{R}^{8\times 1}$. The update of $\boldsymbol{B}_k$ takes such a strategy

$$\boldsymbol{B}_k = \left(\boldsymbol{I} - \frac{\boldsymbol{\delta}_k \boldsymbol{\gamma}_k^{\top}}{\boldsymbol{\delta}_k^{\top} \boldsymbol{\gamma}_k}\right) \boldsymbol{B}_{k-1} \left(\boldsymbol{I} - \frac{\boldsymbol{\gamma}_k \boldsymbol{\delta}_k^{\top}}{\boldsymbol{\delta}_k^{\top} \boldsymbol{\gamma}_k}\right) + \frac{\boldsymbol{\delta}_k \boldsymbol{\delta}_k^{\top}}{\boldsymbol{\delta}_k^{\top} \boldsymbol{\gamma}_k}, \tag{7}$$

with $\boldsymbol{\delta}_k = \boldsymbol{\theta}_k - \boldsymbol{\theta}_{k-1}$ and $\boldsymbol{\gamma}_k = \boldsymbol{g}_k - \boldsymbol{g}_{k-1}$, which is known as BFGS update strategy [32]. In addition, $\boldsymbol{g}_k$ can be obtained as

$$\boldsymbol{g}_k = -\frac{\partial \boldsymbol{V}\left(\boldsymbol{\theta}_k;\boldsymbol{u}\right)^{\top}}{\partial \boldsymbol{\theta}_k} \boldsymbol{Q}^{-1} \left[\boldsymbol{y} - \boldsymbol{V}\left(\boldsymbol{\theta}_k;\boldsymbol{u}\right)\right] + \boldsymbol{P}^{-1}\left(\boldsymbol{\theta}_k - \boldsymbol{m}\right),$$

where each column of $\frac{\partial \boldsymbol{V}(\boldsymbol{\theta};\boldsymbol{u})}{\partial \boldsymbol{\theta}} \in \mathbb{R}^{N\times 8}$ is given by

$$\frac{\partial \boldsymbol{V}\left(\boldsymbol{\theta};\boldsymbol{u}\right)}{\partial \theta_1} = \boldsymbol{\Sigma} \circ \frac{q^{-1} - \theta_3 q^{-2}}{1 - (1+\theta_3)q^{-1} + \theta_3 q^{-2}} \boldsymbol{u},$$

$$\frac{\partial \boldsymbol{V}\left(\boldsymbol{\theta};\boldsymbol{u}\right)}{\partial \theta_2} = \boldsymbol{\Sigma} \circ \frac{q^{-1} - q^{-2}}{1 - (1+\theta_3)q^{-1} + \theta_3 q^{-2}} \boldsymbol{u},$$

$$\frac{\partial \boldsymbol{V}\left(\boldsymbol{\theta};\boldsymbol{u}\right)}{\partial \theta_3} = \boldsymbol{\Sigma} \circ \frac{\theta_2 q^{-2} - 2\theta_2 q^{-3} + \theta_2 q^{-4}}{\left(1 - (1+\theta_3)q^{-1} + \theta_3 q^{-2}\right)^2} \boldsymbol{u},$$

$$\frac{\partial \boldsymbol{V}\left(\boldsymbol{\theta};\boldsymbol{u}\right)}{\partial \theta_i} = \boldsymbol{x}^{\circ(i-3)} - \boldsymbol{x}^{\circ 5} \text{ for } i = 4, \ldots, 7,$$

$$\frac{\partial \boldsymbol{V}\left(\boldsymbol{\theta};\boldsymbol{u}\right)}{\partial \theta_8} = \boldsymbol{u},$$

with

$$\boldsymbol{x} = G_1(q,\boldsymbol{\theta})\boldsymbol{u} + G_2(q) V_s(0) \mathbf{1},$$

$$\boldsymbol{\Sigma} = \sum_{i=4}^{7} (i-3)\theta_i \boldsymbol{x}^{\circ(i-4)} + 5\left(\overline{V} - \underline{V} - \sum_{i=4}^{7} \theta_i\right) \boldsymbol{x}^{\circ 4}.$$

TABLE I: A quasi-Newton method for MAP estimation.

Given initial iterate $\boldsymbol{\theta}_0$ and convergence tolerance ε
repeat
  Compute the gradient vector $\boldsymbol{g}_k$
  if $k = 0$ **then**
    Compute $\boldsymbol{B}_0 = 0.001 \frac{1}{\|\boldsymbol{g}_0\|} \boldsymbol{I}$
  else
    Compute $\boldsymbol{B}_k$ based on (7)
  end if
  Set search direction $\boldsymbol{s}_k = -\boldsymbol{B}_k \boldsymbol{g}_k$
  Find step length λ_k satisfying the Wolfe conditions (8), where $c_1 = 10^{-6}$ and $c_2 = 0.9$
  Set new iterate $\boldsymbol{\theta}_{k+1} = \boldsymbol{\theta}_k + \lambda_k \boldsymbol{s}_k$
until $J(\boldsymbol{\theta}_k)$ converges
return $\hat{\boldsymbol{\theta}} = \boldsymbol{\theta}_k$

Here, $\boldsymbol{x} \circ \boldsymbol{u}$ denotes the Hadamard product of $\boldsymbol{x}$ and $\boldsymbol{u}$, $\boldsymbol{x}^{\circ 2}$ denotes the Hadamard power with $\boldsymbol{x}^{\circ 2} = \boldsymbol{x} \circ \boldsymbol{x}$, and $\mathbf{1} \in \mathbb{R}^{N\times 1}$ denotes a column vector with each element equal to one. Finally, note that λ_k needs to be chosen carefully to make $J(\boldsymbol{\theta})$ decrease monotonically. We can use the Wolfe conditions and let λ_k be selected such that

$$J\left(\boldsymbol{\theta}_k + \lambda_k \boldsymbol{s}_k\right) \leq J\left(\boldsymbol{\theta}_k\right) + c_1 \lambda_k \boldsymbol{g}_k^{\top} \boldsymbol{s}_k, \tag{8a}$$

$$\nabla J\left(\boldsymbol{\theta}_k + \lambda_k \boldsymbol{s}_k\right)^{\top} \boldsymbol{s}_k \geq c_2 \nabla J\left(\boldsymbol{\theta}_k\right)^{\top} \boldsymbol{s}_k, \tag{8b}$$

with $0 < c_1 < c_2 < 1$. In practice, c_1 is set to be quite small, e.g., $c_1 = 10^{-6}$, and c_2 is typically set to be 0.9 for the quasi-Newton method. As for selecting λ_k satisfying (8), a simple implementation is to start it with a small value, say $\lambda_k = 1$. If the Wolfe conditions are not met, reduce it and check again. For more information about λ_k selection, the interested reader can refer to [32]. Summarizing the above, we outline the computational algorithm in Table I.

Remark 1: The proposed approach requires some prior knowledge of the parameters to be available. One can develop such a prior knowledge in several ways in practice. First, R_0 can be roughly estimated using the voltage drop at the beginning of the discharge, to which it is a main contributor. Second, one can derive a rough range for $C_b + C_s$ if a battery's capacity is approximately known. Finally, as the parameters of batteries of the same kind and brand are usually close, one can use the parameter estimates obtained from one battery as prior knowledge for another.

IV. Experimental Validation

This section evaluates the effectiveness of the identification approach in the real-world application.

Our experiments were conducted on a PEC® SBT4050 battery tester. Using this facility, charging/discharging tests were performed on a Panasonic NCR18650B Li-ion battery cell, which has a rated capacity of 3 Ah. In one test, the battery was discharged from full capacity by a variable current profile, which is based on the Urban Dynamometer Driving Schedule (UDDS) [33] and adjusted to fall between 0 A and 3 A, see Figure 3(a). The obtained voltage profile

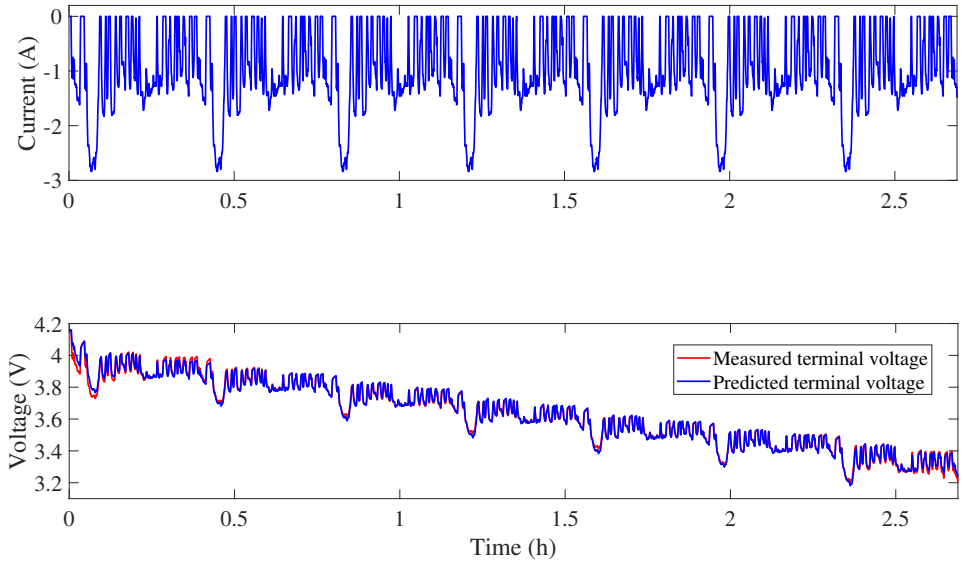

(b) Comparison between measured terminal voltage and predicted terminal voltage.

Fig. 3: Parameter identification using experimental current/voltage data.

TABLE II: Parameter identification results from experimental current/voltage data.

Name	$\breve{\alpha}_1$	$\breve{\alpha}_2$	$\breve{\alpha}_3$	β_1	β_2	β_3	β_4	R_0
$\boldsymbol{\theta}_{\text{guess}}$	9.0777×10^{-5}	8.9135×10^{-4}	0.9640	1	1	1	1	0.08
$\boldsymbol{m}$	9.0777×10^{-5}	8.9135×10^{-4}	0.9640	-	-	-	-	0.08
$\text{diag}(\boldsymbol{P})$	$(0.01 \times m_1)^2$	$(0.15 \times m_2)^2$	$(0.15 \times m_3)^2$	-	-	-	-	$(0.15 \times m_8)^2$
$\hat{\boldsymbol{\theta}}$	9.3973×10^{-5}	9.5673×10^{-4}	0.9811	2.793	-10.993	25.92	-27.43	0.0712

is shown in Figure 3(b) (see the red curve). The sampling time interval Δt was 1 s, the cut-off voltage $\underline{V}$ and $\overline{V}$ was 3.2 V and 4.16 V, respectively. We applied the proposed approach to the collected current/voltage data to identify the parameters. The measurement noise is assumed to be white Gaussian with covariance $\sigma = 10^{-2}$. The initial guess, selected $\boldsymbol{m}$ and $\boldsymbol{P}$, is summarized in Table II. Note that since $\breve{\alpha}_1$ is inversely proportional to $C_b + C_s$ that can be accessed from the battery's full capacity, the initial guess of $\breve{\alpha}_1$ can be very accurate and thus assigned with high confidence, i.e., the corresponding element in $\boldsymbol{P}$ is set to be $(0.01 \times m_1)^2$. With the above setting, parameter estimates are obtained and summarized in Table II. Further, estimates of C_b, C_s and R_b are also calculated, which turns out to be $C_b = 9,697$ F, $C_s = 943.5$ F, and $R_b = 0.06\ \Omega$. The voltage prediction is made using the parameter estimates and compared against the measured voltage in Figure 3(b). One can observe an excellent agreement between them. In addition, it will be interesting to compare the estimated SoC-OCV curve with the true one of the battery. As aforementioned, $\text{OCV} = h(\text{SoC})$ for the NDC model. It is identified here as

$$\text{OCV} = 3.2 + 2.793 \cdot \text{SoC} - 10.993 \cdot \text{SoC}^2 + 25.92 \cdot \text{SoC}^3 - 27.43 \cdot \text{SoC}^4 + 10.67 \cdot \text{SoC}^5.$$

Figure 4 compares it with the SoC-OCV curve obtained experimentally by discharging the battery from full capacity to a cut-off voltage 3.2 V using a small current of 0.1 A.

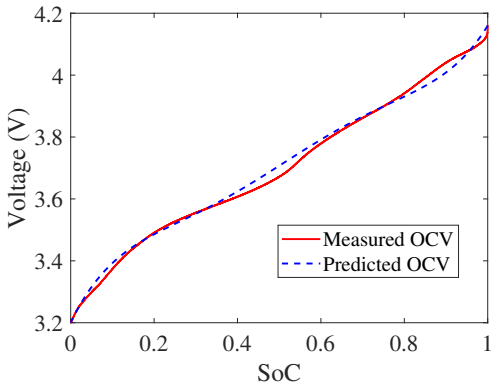

Fig. 4: Comparison between measured and predicted OCV.

It is seen that the identified SoC-OCV curve is very close to the actual one. All the results above show the parameter estimates are reasonable and that the identification method introduced in Section III is effective.

V. Conclusion

This paper deals with parameter identification for the NDC model proposed in our previous work. The NDC model is structurally similar to a Wiener system as it consists of a linear dynamic subsystem and a nonlinear static subsystem in cascade. Known as a challenging problem, Wiener system

identification can often easily fall victim to nonconvexity and local minima due to the model's nonlinearity. To address this issue, we proposed to use MAP estimation so as to incorporate some prior knowledge about the unknown parameters into the design of parameter estimation. Based on this idea, we developed a parameter estimation approach for the NDC model. We validated the approach through experiments, consistently observing its effectiveness in producing accurate estimation. The proposed approach can advantageously estimate all the model parameters in one shot, imposes no restrictions on the current profiles, and is more capable of ensuring physically reasonable estimates to be obtained. The notion of MAP-based Wiener system identification can also find prospective use in many other applications.

REFERENCES

[1] N. Tian, H. Fang, and J. Chen, "A new nonlinear double-capacitor model for rechargeable batteries," in *IECON 2018-44th Annual Conference of the IEEE Industrial Electronics Society*. IEEE, 2018, pp. 1613–1618.

[2] B. Schweighofer, K. M. Raab, and G. Brasseur, "Modeling of high power automotive batteries by the use of an automated test system," *IEEE Transactions on Instrumentation and Measurement*, vol. 52, no. 4, pp. 1087–1091, 2003.

[3] S. Abu-Sharkh and D. Doerffel, "Rapid test and non-linear model characterisation of solid-state lithium-ion batteries," *Journal of Power Sources*, vol. 130, no. 1, pp. 266–274, 2004.

[4] A. Fairweather, M. Foster, and D. Stone, "Battery parameter identification with Pseudo Random Binary Sequence excitation (PRBS)," *Journal of Power Sources*, vol. 196, no. 22, pp. 9398–9406, 2011.

[5] M. Dubarry and B. Y. Liaw, "Development of a universal modeling tool for rechargeable lithium batteries," *Journal of Power Sources*, vol. 174, no. 2, pp. 856–860, 2007.

[6] H. He, R. Xiong, X. Zhang, F. Sun, and J. Fan, "State-of-charge estimation of the lithium-ion battery using an adaptive extended Kalman filter based on an improved Thevenin model," *IEEE Transactions on Vehicular Technology*, vol. 60, no. 4, pp. 1461–1469, 2011.

[7] Y. Tian, B. Xia, W. Sun, Z. Xu, and W. Zheng, "A modified model based state of charge estimation of power lithium-ion batteries using unscented Kalman filter," *Journal of Power Sources*, vol. 270, pp. 619–626, 2014.

[8] P. Mauracher and E. Karden, "Dynamic modelling of lead/acid batteries using impedance spectroscopy for parameter identification," *Journal of Power Sources*, vol. 67, no. 1-2, pp. 69–84, 1997.

[9] K. Goebel, B. Saha, A. Saxena, J. R. Celaya, and J. P. Christophersen, "Prognostics in battery health management," *IEEE Instrumentation & Measurement Magazine*, vol. 11, no. 4, 2008.

[10] C. Birkl and D. Howey, "Model identification and parameter estimation for $LiFePO_4$ batteries," in *Proceedings of IET Hybrid and Electric Vehicles Conference*, 2013, pp. 1–6.

[11] T. Hu and H. Jung, "Simple algorithms for determining parameters of circuit models for charging/discharging batteries," *Journal of Power Sources*, vol. 233, pp. 14–22, 2013.

[12] M. Sitterly, L. Y. Wang, G. G. Yin, and C. Wang, "Enhanced identification of battery models for real-time battery management," *IEEE Transactions on Sustainable Energy*, vol. 2, no. 3, pp. 300–308, 2011.

[13] G. K. Prasad and C. D. Rahn, "Model based identification of aging parameters in lithium ion batteries," *Journal of Power Sources*, vol. 232, pp. 79–85, 2013.

[14] T. Feng, L. Yang, X. Zhao, H. Zhang, and J. Qiang, "Online identification of lithium-ion battery parameters based on an improved equivalent-circuit model and its implementation on battery state-of-power prediction," *Journal of Power Sources*, vol. 281, pp. 192–203, 2015.

[15] Z. He, G. Yang, and L. Lu, "A parameter identification method for dynamics of lithium iron phosphate batteries based on step-change current curves and constant current curves," *Energies*, vol. 9, no. 6, p. 444, 2016.

[16] J. Yang, B. Xia, Y. Shang, W. Huang, and C. Mi, "Improved battery parameter estimation method considering operating scenarios for HEV/EV applications," *Energies*, vol. 10, no. 1, p. 5, 2016.

[17] N. Tian, Y. Wang, J. Chen, and H. Fang, "On parameter identification of an equivalent circuit model for lithium-ion batteries," in *IEEE Conference on Control Technology and Applications*, 2017, pp. 187–192.

[18] Y. Jiang, B. Xia, X. Zhao, T. Nguyen, C. Mi, and R. A. de Callafon, "Data-based fractional differential models for non-linear dynamic modeling of a lithium-ion battery," *Energy*, vol. 135, pp. 171–181, 2017.

[19] Y. Hu and S. Yurkovich, "Linear parameter varying battery model identification using subspace methods," *Journal of Power Sources*, vol. 196, no. 5, pp. 2913–2923, 2011.

[20] Y. Li, C. Liao, L. Wang, L. Wang, and D. Xu, "Subspace-based modeling and parameter identification of lithium-ion batteries," *International Journal of Energy Research*, vol. 38, no. 8, pp. 1024–1038, 2014.

[21] J. C. Forman, S. J. Moura, J. L. Stein, and H. K. Fathy, "Genetic identification and fisher identifiability analysis of the Doyle–Fuller–Newman model from experimental cycling of a LiFePO4 cell," *Journal of Power Sources*, vol. 210, pp. 263 – 275, 2012.

[22] L. Zhang, L. Wang, G. Hinds, C. Lyu, J. Zheng, and J. Li, "Multi-objective optimization of lithium-ion battery model using genetic algorithm approach," *Journal of Power Sources*, vol. 270, pp. 367–378, 2014.

[23] M. A. Rahman, S. Anwar, and A. Izadian, "Electrochemical model parameter identification of a lithium-ion battery using particle swarm optimization method," *Journal of Power Sources*, vol. 307, pp. 86–97, 2016.

[24] Z. Yu, L. Xiao, H. Li, X. Zhu, and R. Huai, "Model parameter identification for lithium batteries using the coevolutionary particle swarm optimization method," *IEEE Trans. Ind. Electron*, vol. 64, no. 7, pp. 5690–5700, 2017.

[25] M. J. Rothenberger, D. J. Docimo, M. Ghanaatpishe, and H. K. Fathy, "Genetic optimization and experimental validation of a test cycle that maximizes parameter identifiability for a Li-ion equivalent-circuit battery model," *Journal of Energy Storage*, vol. 4, pp. 156 – 166, 2015.

[26] S. Park, D. Kato, Z. Gima, R. Klein, and S. Moura, "Optimal input design for parameter identification in an electrochemical Li-ion battery model," in *Proceedings of American Control Conference*, 2018, pp. 2300–2305.

[27] F. Giri and E.-W. Bai, *Block-Oriented Nonlinear System Identification*. Springer, 2010, vol. 1.

[28] A. Hagenblad, L. Ljung, and A. Wills, "Maximum likelihood identification of Wiener models," *Automatica*, vol. 44, no. 11, pp. 2697 – 2705, 2008.

[29] L. Vanbeylen, R. Pintelon, and J. Schoukens, "Blind maximum-likelihood identification of Wiener systems," *IEEE Transactions on Signal Processing*, vol. 57, no. 8, pp. 3017–3029, 2009.

[30] A. Hagenblad, "Aspects of the identification of Wiener models," Ph.D. dissertation, Linköping University, 1999.

[31] A. Hagenblad, L. Ljung, and A. Wills, "Maximum likelihood identification of Wiener models," *Automatica*, vol. 44, no. 11, pp. 2697–2705, 2008.

[32] S. Wright and J. Nocedal, "Numerical optimization," *Springer Science*, vol. 35, no. 67-68, p. 7, 1999.

[33] "The EPA Urban Dynamometer Driving Schedule (UDDS) [Online]," Available: https://www.epa.gov/sites/production/files/2015-10/uddscol.txt.